Mon. Not. R. Astron. Soc. **360,** 655–661 (2005) doi:10.1111/j.1365-2966.2005.09054.x

The intermediate-age open clusters Ruprecht 4, Ruprecht 7 and Pismis 15

G. Carraro,[1,2★]† D. Geisler,[3] G. Baume,[4] R. Vázquez[4] and A. Moitinho[5]

[1]*Departamento de Astronomía, Universidad de Chile, Casilla 36-D, Santiago, Chile*
[2]*Astronomy Department, Yale University, PO Box 208101, New Haven, CT 06520-8101, USA*
[3]*Universidad de Concepción, Departamento de Fisica, Casilla 160-C, Concepción, Chile*
[4]*Facultad de Ciencias Astronómicas y Geofísicas de la UNLP, IALP-CONICET, Paseo del Bosque s/n, La Plata, Argentina*
[5]*CAAUL, Observatório Astronómico de Lisboa, Tapada da Ajuda, 1349-018 Lisboa, Portugal*

Accepted 2005 March 24. Received 2005 March 23; in original form 2005 February 15

ABSTRACT

We report on *BVI* CCD photometry to $V = 22.0$ for three fields centred on the region of the Galactic star clusters Ruprecht 4, Ruprecht 7 and Pismis 15 and on three displaced control fields. Ruprecht 4 and Pismis 15 have never been studied before, and we provide, for the first time, estimates of their fundamental parameters, namely, radial extent, age, distance and reddening. Ruprecht 7 (Berkeley 33), however, was studied by Mazur, Kaluzny & Krzeminski. We find that the three clusters are all of intermediate age (0.8–1.3 Gyr), and with a metallicity close to or lower than solar.

Key words: open clusters and associations: general – open clusters and associations: individual: Ruprecht 4 – open clusters and associations: individual: Ruprecht 7 – open clusters and associations: individual: Pismis 15.

1 INTRODUCTION

This paper is part of a series dedicated to the study of the open cluster population in the third Galactic quadrant, and aims at addressing fundamental questions like the structure of the spiral arms in this quadrant, and the precise definition of the Galactic disc radial abundance gradient outside the solar circle. A more detailed illustration of the motivations of this project is given in Moitinho (2001) and Baume et al. (2004). Here we concentrate on three intermediate-age clusters (about the age of the Hyades – 600 Myr – or older), Ruprecht 4, Ruprecht 7 and Pismis 15 (see Table 1), for which we provide new photometric data and try to clarify their nature and to derive the first estimates of their fundamental parameters.

The layout of the paper is as follows. Section 2 illustrates the observation and reduction strategies. An analysis of the geometrical structure and star counts in the field of the clusters is presented in Section 3, whereas a discussion of the colour–magnitude diagrams (CMD) is given in Section 4. Section 5 deals with the determination of cluster reddening, distance and age and, finally, Section 6 summarizes our findings.

2 OBSERVATIONS AND DATA REDUCTION

CCD *BVI* observations were carried out with the CCD camera onboard the 1-m telescope at Cerro Tololo Interamerican Observatory (CTIO, Chile), on the nights of 2004 December 13 and 15. With a pixel size of 0.469 arcsec, and a CCD size of 512 × 512 pixels, this samples a 4.1 × 4.1 arcmin^2 field on the sky.

The details of the observations are listed in Table 2 where the observed fields are reported together with the exposure times, the average seeing values and the range of airmasses during the observations. Figs 1–3 show finding charts in the area of Ruprecht 4, Ruprecht 7 and Pismis 15, respectively.

The data have been reduced with the IRAF packages CCDRED, DAOPHOT, ALLSTAR and PHOTCAL using the point spread function (PSF) method (Stetson 1987). The two nights turned out to be photometric and very stable, and therefore we derived calibration equations for all the 130 standard stars observed during the two nights in the Landolt (1992) fields SA 95-41, PG 0231+051, Rubin 149, Rubin 152, T phe and SA 98-670 (see Table 2 for details). Together with the clusters, we observed three control fields 20 arcmin apart from the nominal cluster centres to deal with field star contamination. Exposure of 600 s in *V* and *I* were secured for these fields.

The calibration equations turned out to be of the form:

$$b = B + b_1 + b_2 \times X + b_3\,(B - V),$$
$$v = V + v_1 + v_2 \times X + v_3\,(B - V),$$
$$v = V + v_{1,i} + v_{2,i} \times X + v_{3,i} \times (V - I),$$
$$i = I + i_1 + i_2 \times X + i_3\,(V - I),$$

where *BVI* are standard magnitudes, b, v, i are the instrumental magnitudes and X is the airmass; all the coefficient values are reported in Table 3. The standard stars in these fields provide a very good colour coverage. The final rms of the calibration are 0.039, 0.034 and 0.033 for the *B*, *V* and *I* filters, respectively.

We generally used the third equation to calibrate the *V* magnitude in order to get the same magnitude depth both in the cluster and in

★On leave from Dipartimento di Astronomia, Università di Padova, Vicolo Osservatorio 2, I-35122, Padova, Italy.
†E-mail: gcarraro@das.uchile.cl

Table 1. Basic parameters of the clusters under investigation. Coordinates are for J2000.0 equinox.

Name	RA	Dec.	l	b
Ruprecht 4	$06^h48^m59^s$	$-10°31'10''$	222.°04	−5.°31
Ruprecht 7	$06^h57^m52^s$	$-13°13'25''$	225.°44	−4.°58
Pismis 15	$09^h34^m45^s$	$-48°02'19''$	272.°49	+2.°86

Table 2. Journal of observations of Ruprecht 4, Ruprecht 7 and Pismis 15 and standard star fields (2004 December 13 and 15).

Field	Filter	Exposure time (s)	Seeing (arcsec)	Airmass
Ruprecht 4	*B*	120 1200	1.2	1.12–1.20
	V	30 600	1.3	1.12–1.20
	I	30 600	1.2	1.12–1.20
Ruprecht 7	*B*	120 1200	1.2	1.12–1.20
	V	30 600	1.3	1.12–1.20
	I	30 600	1.2	1.12–1.20
Pismis 15	*B*	120 1200	1.2	1.12–1.20
	V	30 600	1.3	1.12–1.20
	I	30 600	1.2	1.12–1.20
SA 98-671	*B*	3 × 120	1.2	1.24–1.26
	V	3 × 40	1.4	1.24–1.26
	I	3 × 20	1.4	1.24–1.26
PG 0231+051	*B*	3 × 120	1.2	1.20–2.04
	V	3 × 40	1.5	1.20–2.04
	I	3 × 20	1.5	1.20–2.04
T Phe	*B*	3 × 120	1.2	1.04–1.34
	V	3 × 40	1.3	1.04–1.34
	I	3 × 20	1.3	1.04–1.34
Rubin 152	*B*	3 × 120	1.3	1.33–1.80
	V	3 × 40	1.2	1.33–1.80
	I	3 × 20	1.2	1.33–1.80
Rubin 149	*B*	3 × 120	1.1	1.21–1.96
	V	3 × 40	1.2	1.21–1.96
	I	3 × 20	1.2	1.21–1.96
SA 95-41	*B*	3 × 120	1.2	1.05–1.48
	V	3 × 40	1.2	1.05–1.48
	I	3 × 20	1.1	1.05–1.48

the field. Photometric errors have been estimated following Patat & Carraro (2001). It turns out that stars brighter than $V \approx 22$ mag have internal (ALLSTAR output) photometric errors lower than 0.10 mag in magnitude and lower than 0.18 mag in colour, as one can readily see by inspecting Fig. 4. There the trend of errors in colours and magnitude are reported against the V magnitude.

The final photometric catalogue for Ruprecht 4, Ruprecht 7 and Pismis 15 (coordinates, B, V and I magnitudes and errors) consists of 953, 769 and 1007 stars, respectively, and are made available in electronic form at the WEBDA[1] site maintained by J.-C. Mermilliod.

[1] http://obswww.unige.ch/webda/navigation.html

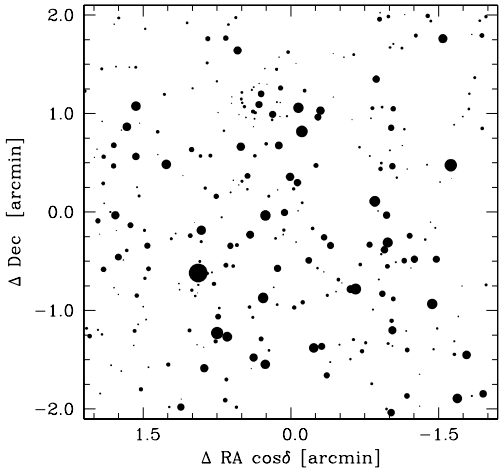

Figure 1. *V* finding charts in the region of the open cluster Ruprecht 4. The sizes of the dots are proportional to the star magnitude. North is up, east on the left, and the covered area is 4.1 × 4.1 arcmin^2.

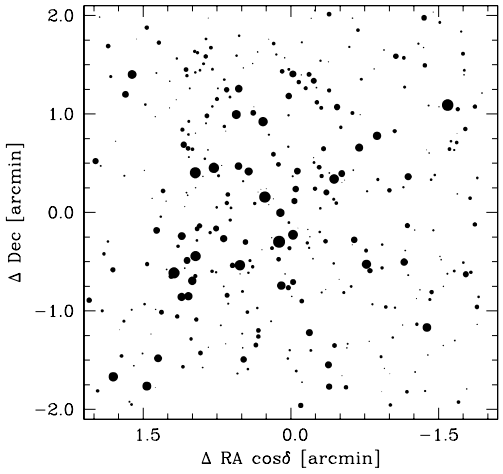

Figure 2. *V* finding chart in the region of the open cluster Ruprecht 7. The sizes of the dots are proportional to the star magnitude. North is up, east on the left, and the covered area is 4.1 × 4.1 arcmin^2.

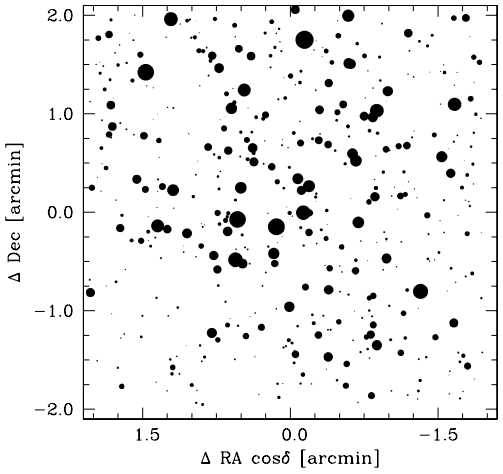

Figure 3. *V* finding chart in the region of the open cluster Pismis 15. The sizes of the dots are proportional to the star magnitude. North is up, east on the left, and the covered area is 4.1 × 4.1 arcmin^2.

Table 3. Coefficients of the calibration equations.

$b_1 = 3.465 \pm 0.009$	$b_2 = 0.25 \pm 0.02$	$b_3 = -0.145 \pm 0.008$
$v_1 = 3.244 \pm 0.005$	$v_2 = 0.16 \pm 0.02$	$v_3 = 0.021 \pm 0.005$
$i_1 = 4.097 \pm 0.005$	$i_2 = 0.08 \pm 0.02$	$i_3 = 0.006 \pm 0.005$
$i_1 = 4.097 \pm 0.005$	$i_2 = 0.08 \pm 0.02$	$i_3 = 0.006 \pm 0.005$

3 STAR COUNTS AND CLUSTER SIZE

Since our photometry covers the area of each cluster entirely we performed star counts to obtain an improved estimate of the cluster size. We derived the surface stellar density by performing star counts in concentric rings around the nominal centres of the clusters and then dividing by their respective area. Poisson errors have also been derived and normalized to the corresponding area. The field star contribution has been derived from the control field which we secured for each cluster.

3.1 Ruprecht 4

The final radial density profile for Ruprecht 4 is shown in Fig. 5 as a function of V magnitude. Clearly, the cluster does not appear concentrated, and at the nominal cluster centre we can see a deficiency of stars, which populate a sort of ring-like structure (see also Fig. 1) at 1.5 arcmin from the centre. This is not unusual for open clusters, which in many case are sparse objects.

The cluster seems to be populated by stars of magnitude in the range $15 \leqslant V \leqslant 22$, where it clearly emerges from the background. In this magnitude range the radius is no larger than 1.5 arcmin. We shall adopt the value of 1.5 arcmin as the Ruprecht 4 radius throughout this paper. This estimate is smaller than the value of 4.5 arcmin reported by Dias et al. (2002) for the cluster diameter.

3.2 Ruprecht 7

The final radial density profile for Ruprecht 7 is shown in Fig. 6 as a function of V magnitude. The cluster seems to be populated by stars of magnitude in the range $14 \leqslant V \leqslant 22$, where it clearly emerges from the background. In this magnitude range the radius is no larger than 1.5 arcmin. In conclusion, we adopt the value of 1.5 arcmin as the Ruprecht 7 radius throughout this paper. This estimate is smaller than the value of 4.0 arcmin reported by Dias et al. (2002) for the cluster diameter.

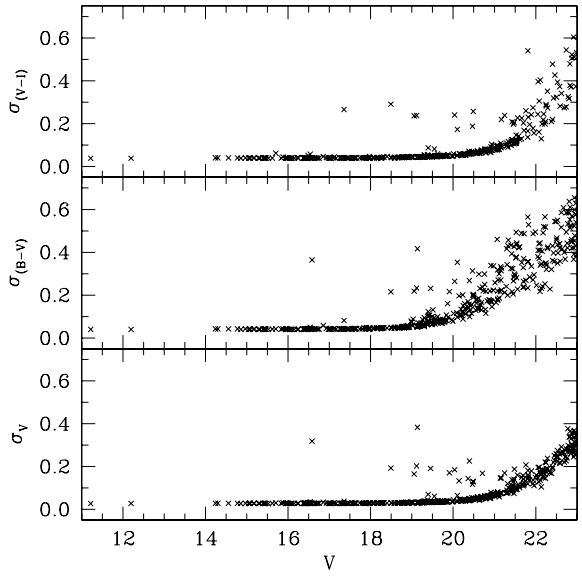

Figure 4. Trend of photometric errors in V, $(B - V)$ and $(V - I)$ as a function of V magnitude.

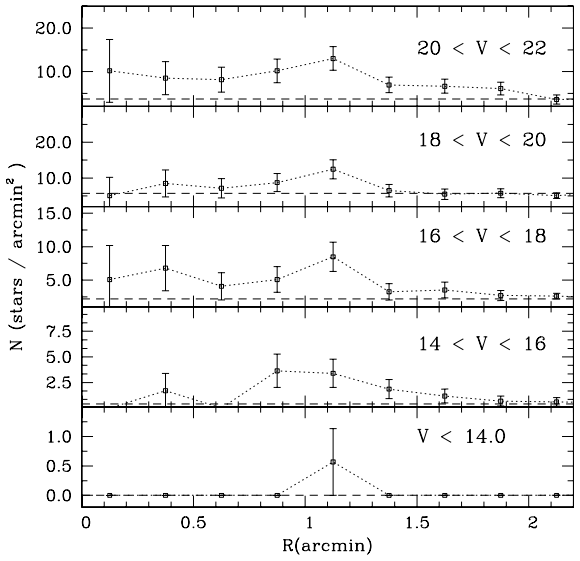

Figure 5. Star counts in the area of Ruprecht 4 as a function of radius and magnitude. The dashed lines represent the level of the control field counts estimated in the surroundings of the cluster in that magnitude range.

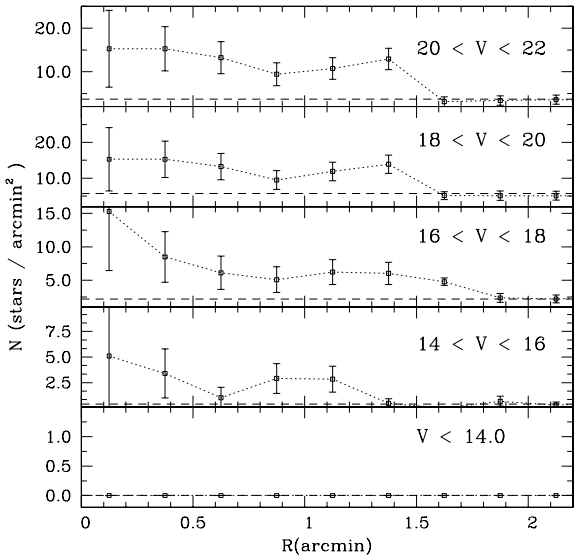

Figure 6. Star counts in the area of Ruprecht 7 as a function of radius and magnitude. The dashed lines represent the level of the control field counts estimated in the surroundings of the cluster in that magnitude range.

3.3 Pismis 15

The final radial density profile for Pismis 15 is shown in Fig. 7 as a function of V magnitude. The cluster seems to be populated by stars of magnitude in the range $14 \leqslant V \leqslant 22$, where it clearly emerges from the background. In this magnitude range the radius is no larger than 1.8 arcmin. In conclusion, we adopt the value of 1.8 arcmin as the Pismis 15 radius throughout this paper. This estimate is in

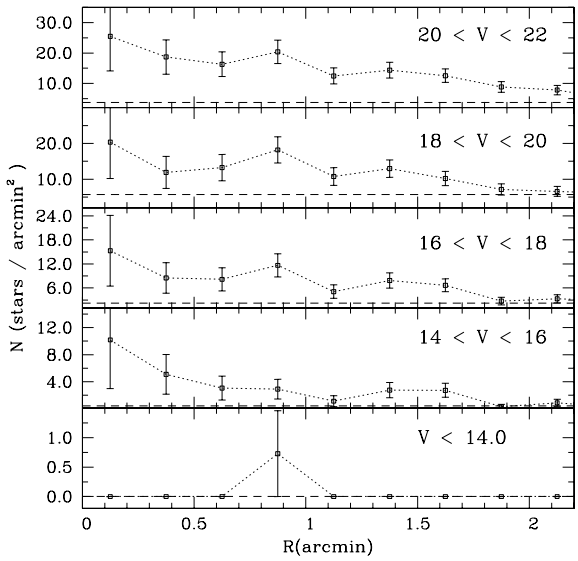

Figure 7. Star counts in the area of Pismis 15 as a function of radius and magnitude. The dashed lines represent the level of the control field counts estimated in the surroundings of the cluster in that magnitude range.

good agreement with the value of 4.0 arcmin reported by Dias et al. (2002) for the cluster diameter.

The estimates we provide for the radius, although reasonable, must be taken as preliminary. In fact the size of the CCD is probably too small to derive conclusive estimates of the cluster sizes. This is particularly true in the case Pismis 15, for which the cluster radius we derived must be considered as a lower limit of the real cluster radius. In fact, while for Ruprecht 4 and 7 the cluster density profile converges toward the field level within the region covered by the CCD, in the case of Pismis 15 the cluster dominates the star counts – at least for the faintest stars – up to the border of the region we covered. Larger field coverage is necessary in this case to derive a firm estimate of the cluster radius.

4 THE COLOUR–MAGNITUDE DIAGRAMS

In Fig. 8 we present the CMDs we obtained for the three clusters under investigation. In this figure the open cluster Ruprecht 4 is shown together with the corresponding control field in the lower panels, whereas Ruprecht 7 and Pismis 15 are presented in the middle and upper panels, respectively. The control fields help us to interpret these CMDs, which are clearly dominated by foreground star contamination.

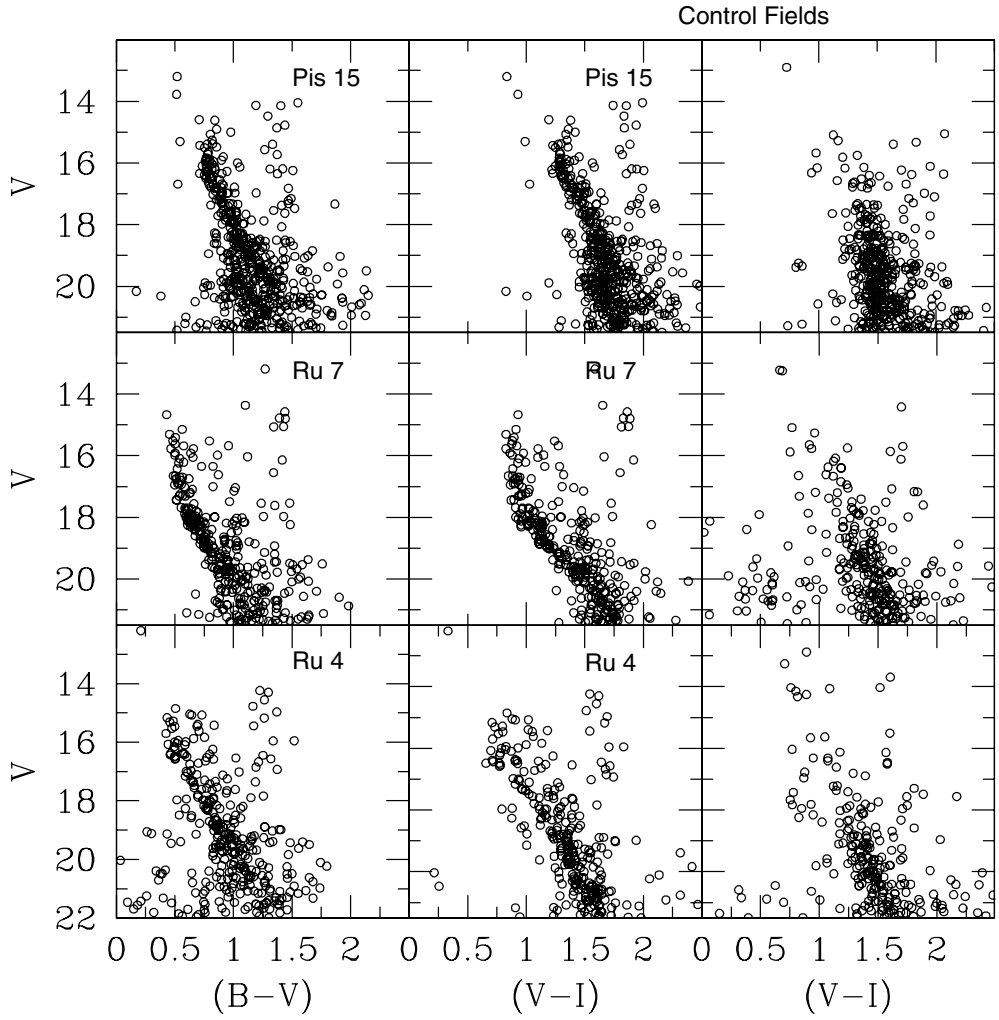

Figure 8. V versus $(B-V)$ (left panels) and V versus $(V-I)$ (middle panels) CMDs of Ruprecht 4 (lower panels), Ruprecht 15 (middle panels) and Pismis 15 (upper panels) and corresponding control fields (right panels). We include all stars in each field.

4.1 Ruprecht 4

This cluster is presented in the lower panels of Fig. 8. It exhibits a main sequence (MS) extending from $V = 16$, where the turn-off point (TO) is located down to $V = 22$. This MS is very wide, a fact that we ascribe to the increasing photometric error at increasing magnitude, the field star contamination, and the presence of a sizeable binary star population, which mainly enlarge the MS toward red colours. In particular the effect of a significant binary population is known to affect the MS and TO shape, which appear at first glance confused (see for comparison the CMDs in the middle and upper panels; for reference see also Meynet, Mermilliod & Maeder 1993).

However, the reality of this cluster seems to be secured by the shape of the MS with respect to the control field MS, whose population sharply decreases at $V = 18$. Besides, the cluster MS is significantly bluer and more tilted than the field MS, which derives from the superposition of stars of different reddening located at all distances between the cluster and the Sun. Other interesting evidence it the possible presence of a clump of stars at $V = 15$, which does not have a clear counterpart in the field, and which makes the cluster an intermediate-age cluster. In fact if we use the age calibration from Carraro & Chiosi (1994), for a ΔV (say the magnitude difference between the red clump ant the TO) of 1 mag, we infer an age of around a billion years. This estimate does not take into account the cluster metallicity, and therefore is simply a guess. In the following we shall provide a more robust estimate of the age through a detailed comparison with theoretical isochrones.

4.2 Ruprecht 7

The open cluster Ruprecht 7 is presented in the middle panels of Fig. 8. The interpretation of this CMD seems much easier than the previous one. Here the MS is more evident, the TO is located at $V \approx 15.5$, and the clump at $V \approx 15$, thus implying a rough estimate for the age around 0.5 billion years. The overall morphology of the CMDs is so different from the field CMD that it leaves no doubt about the reality of the cluster. Also in this case the distribution of the stars in the red edge of the MS suggests a probably binary star population. Both Ruprecht 4 and Ruprecht 7 have a clump mean magnitude $V = 15$. According to Salaris & Girardi (2002), this implies a common distance modulus $(m - M)$ of about 15 mag.

4.3 Pismis 15

The open cluster Pismis 15 is finally presented in the upper panels of Fig. 8. The TO is located at $V \approx 16$, and the clump at $V \approx 14.5$, thus implying a rough estimate for the age of around 1.5 billion years. The overall morphology of the CMDs is also in this case very different from the field CMD so this is a bona fide cluster. A word of caution is mandatory because the precise clump position is affected by field star contamination in the form of a tail of stars which connects the clump with the MS at $V = 18$. Again, the control field helps us to interpret the CMD. Indeed also in the control field there is a vertical sequence detaching from the MS at $V = 18$, which, however, stops at $V = 15$, supporting the interpretation of the 5–6 bright red stars as clump stars with mean $V = 14.5$. This suggests that Pismis 15 might be somewhat closer to the Sun than the other two clusters.

5 DERIVING THE FUNDAMENTAL PARAMETERS OF CLUSTERS

In this section we are going to perform a detailed comparison of the star distribution in the cluster CMDs with theoretical isochrones. We adopt in this study the Padova library from Girardi et al. (2000). This comparison is clearly not an easy exercise. In fact the detailed shape and position of the various features in the CMD (MS, TO and clump basically) depends mostly on age and metallicity, and then also on reddening and distance. The complex interplay between the various parameters is well known, and we refer to Chiosi, Bertelli & Bressan (1992) and Carraro (2005) as nice examples of the underlying technique.

Our basic strategy is to survey different age and metallicity isochrones attempting to provide the best fit of all the CMD features both in the V versus $(B - V)$ and in the V versus $(V - I)$ CMDs.

Besides, to facilitate the fitting procedure further we shall consider only those stars that lie within the cluster radius as derived in Section 3. Therefore, in the series of Figs 9–11 we shall present the best fit we were able to achieve. Together with the best fit, we could make estimates of uncertainties in the derivation of the basic parameters. These uncertainties simply reflect the range in the basic parameter which allow a reasonable fit to the cluster CMDs. Error estimates are reported in Table 4.

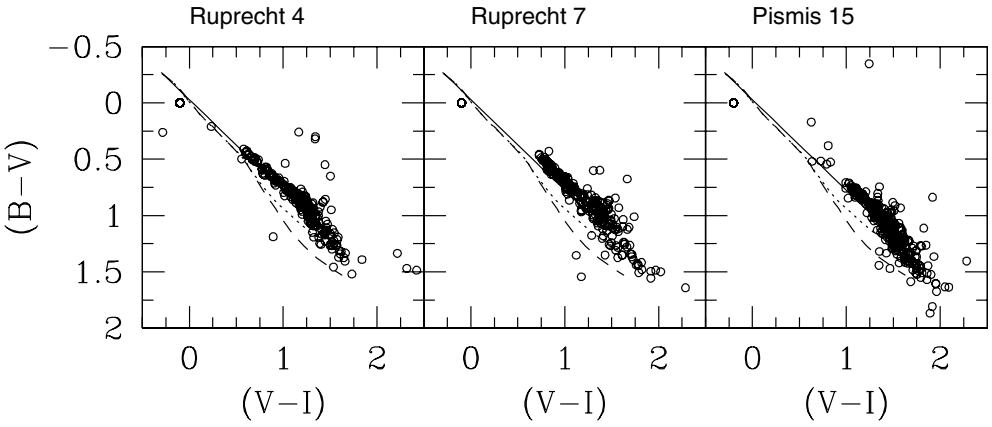

Figure 9. $B - V$ versus $V - I$ diagram for the three clusters. The solid line is the normal reddening law, whereas dashed and dotted lines are the luminosity class III and V ZAMS, respectively. See text for details.

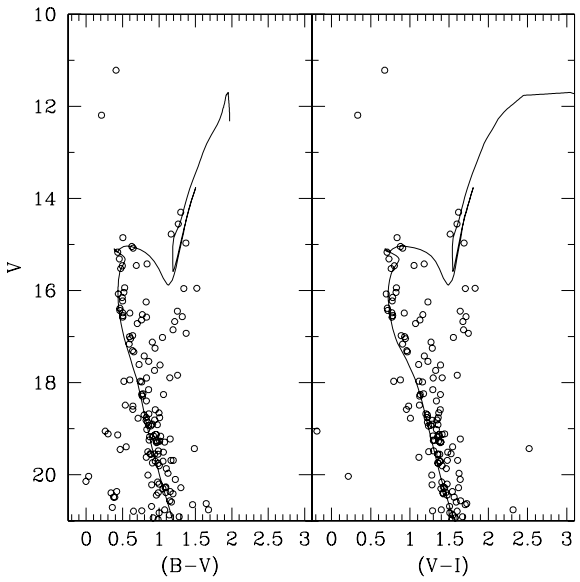

Figure 10. Isochrone solution for Ruprecht 4. The isochrone is for the age of 800 million year and metallicity $Z = 0.008$. The apparent distance modulus is $(m - M) = 14.6$, and the reddening $E(B - V) = 0.36$ and $E(V - I) = 0.50$. See text for more details. Only stars within the derived radius are shown.

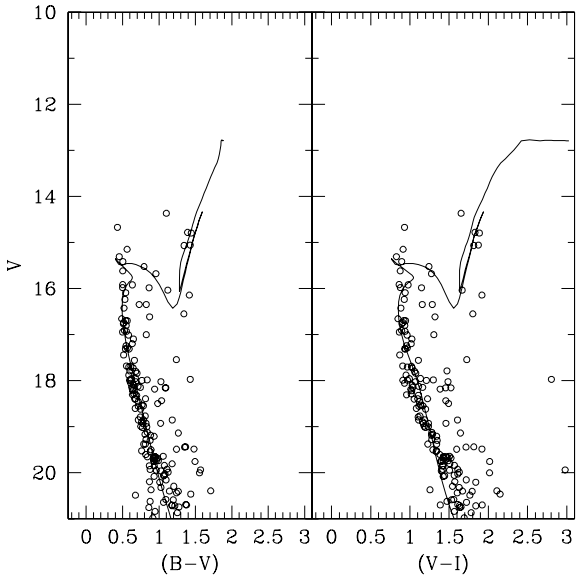

Figure 11. Isochrone solution for Ruprecht 7. The isochrone is for the age of 800 million years and metallicity $Z = 0.019$. The apparent distance modulus is $(m - M) = 15.0$, and the reddening $E(B - V) = 0.30$ and $E(V - I) = 0.47$. See text for more details. Only stars within the derived radius are shown.

Finally, to derive the distances of clusters from reddening and apparent distance modulus, a reddening law must be specified. In Fig. 9 we show that the normal extinction law is valid for all the clusters, and therefore we shall us the relation $Av = 3.1 \times E(B - V)$ to derive the distances of clusters. In detail, the solid line in Fig. 9 is the normal extinction $E(V-) = 1.245 \times E(B - V)$ law from Cousin (1978), whereas the dashed and dotted lines are the luminosity class III and V ZAMS, respectively.

5.1 Ruprecht 4

The isochrone solution for this cluster is discussed in Fig. 10. We obtained the best fit for an age of 800 million years and a metallicity $Z = 0.008$, quite low for an open cluster of this age. The inferred reddening and apparent distance modulus are $E(B - V) = 0.36$ ($E(V - I) = 0.50$) and $(m - M) = 14.6$, respectively. As a consequence the cluster possesses a heliocentric distance of 4.9 kpc, and is located at a Galactocentric distance of 12.0 kpc, assuming 8.5 kpc as the distance of the Sun to the Galactic Centre. Interestingly, this cluster appears to be relatively young but very metal-poor. This is not an isolated case, and Moitinho et al. (2005) reported a similar case, the star cluster NGC 2635. The overall fit is very good, the detailed shape of the MS and TO are nicely reproduced, as is the colour of the clump.

5.2 Ruprecht 7

The isochrone solution for this cluster is discussed in Fig. 11. We obtained the best fit for an age of 800 million years and a metallicity $Z = 0.019$. This metallicity is larger than that proposed by Mazur et al. (1993), which was based on a comparison with the isochrone from Bertelli et al. (1994). The inferred reddening and apparent distance modulus are $E(B - V) = 0.30$ ($E(V - I) = 0.47$) and $(m - M) = 15.0$, respectively. As a consequence the cluster lies at 6.5 kpc from the Sun, and is located at a Galactocentric distance of 13.8 kpc toward the anticentre direction. The overall fit is very good also in this case, the detailed shape of the MS and TO are nicely reproduced, as is the colour of the clump.

With respect to the study by Mazur et al. (1993), we obtain a larger distance. However, both the age and the reddening are compatible with that study. We believe that the larger distance is due to the different isochrone set and mostly to the higher metallicity adopted here for this cluster.

5.3 Pismis 15

The isochrone solution for this cluster is discussed in Fig. 12. We obtained the best fit for an age of 1300 million years and a metallicity $Z = 0.008$. The inferred reddening and apparent distance modulus are $E(B - V) = 0.53$ ($E(V - I) = 0.88$) and $(m - M) = 14.0$, respectively. Therefore the cluster has a heliocentric distance of 2.9 kpc, and is located at a Galactocentric distance of 8.8 kpc. The

Table 4. Fundamental parameters of the studied clusters. The coordinates system is such that the *Y*-axis connects the Sun to the Galactic Centre, while the *X*-axis is perpendicular to that. *Y* is positive toward the Galactic anticentre, and *X* is positive in the first and second Galactic quadrants (Lynga 1982).

Name	Radius (arcmin)	$E(B - V)$	$E(V - I)$	$(m - M)$	$d_\odot$	Y (kpc)	X (kpc)	Z (kpc)	R_{GC} (kpc)	Age (Gyr)	Metallicity
Ruprecht 4	1.5	0.36 ± 0.1	0.50 ± 0.1	14.6 ± 0.2	4.9	−3.6	−3.3	−0.45	12.0	0.8 ± 0.2	0.008 ± 0.005
Ruprecht 7	1.5	0.30 ± 0.1	0.47 ± 0.1	15.0 ± 0.2	7.0	−4.6	−4.6	−0.50	13.8	0.8 ± 0.3	0.019 ± 0.002
Pismis 15	1.8	0.53 ± 0.1	0.88 ± 0.1	14.0 ± 0.2	2.9	0.1	−2.9	0.10	8.8	1.3 ± 0.3	0.008 ± 0.002

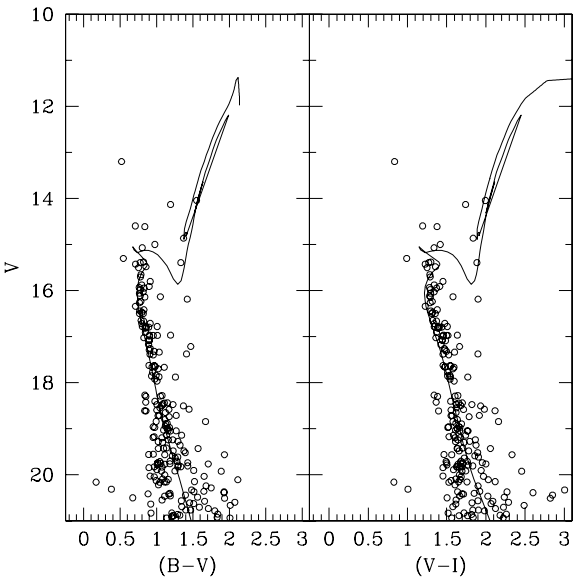

Figure 12. Isochrone solution for Pismis 15. The isochrone is for the age of 1300 million years and metallicity $Z = 0.008$. The apparent distance modulus is $(m - M) = 14.0$, and the reddening $E(B - V) = 0.53$ and $E(V - I) = 0.88$. See text for more details. Only stars within the derived radius are shown.

overall fit is very good also in this case, the detailed shape of the MS and TO are nicely reproduced, as is the colour of the clump.

6 CONCLUSIONS

We have presented the first CCD *BVI* photometric study of the star clusters Ruprecht 4, Ruprecht 7 and Pismis 15. The CMDs we derive allow us to infer estimates of the basic parameters of the clusters, which are summarized in Table 4.

In detail, the fundamental findings of this paper are as follows.

(i) The best-fitting reddening estimates support, within the errors, a normal extinction law toward the three clusters.

(ii) Ruprecht 4 is an intermediate-age open cluster whose position is compatible with the cluster belonging to the local spiral arm.

(iii) Ruprecht 7 is a Hyades-age cluster, although much poorer in metal than that cluster, and is located at almost 14.0 kpc in the anticentre direction, thus being one of the most distant open cluster in the sense of the Galactocentric distance.

(iv) Pismis 15 is an old open cluster located inside the solar ring, with a half than solar metal abundance. The distance we derived and its Galactic coordinates imply that the cluster probably belongs to the Carina spiral arm.

All these clusters are very interesting in the context of the chemical evolution of the Galactic disc (Geisler, Claria & Minniti 1992; Carraro, Ng & Portinari 1998; Friel et al. 2002).

They may be very useful to trace the slope of the Galactic disc radial abundance gradient, which is very poorly sampled in the age range between 0.5 and 2 Gyr (see Friel et al. 2002). If we make use of the provisional photometric estimates presented in this paper, we find that all the clusters basically confirm the most recent slope of the gradient as derive by Friel et al. (2002).

Further studies therefore should concentrate on the confirmation of the metal content of clusters by means of a detailed abundance analysis of the clump stars.

ACKNOWLEDGMENTS

The observations presented in this paper were carried out at the Cerro Tololo Interamerican Observatory CTIO (Chile). CTIO is operated by the Association of Universities for Research in Astronomy, Inc. (AURA), under a cooperative agreement with the National Science Foundation as part of the National Optical Astronomy Observatory (NOAO). The work of GC is supported by Fundación Andes. DG gratefully acknowledges support from the Chilean Centro de Astrofísica FONDAP No. 15010003. This work has also been developed in the framework of the Programa Científico-Tecnológico Argentino-Italiano SECYT-MAE Código: IT/PA03 – UIII/077 – período 2004–2005. This study made use of the Simbad and WEBDA data bases. IRAF is distributed by NOAO, which is operated by AURA under cooperative agreement with the NSF.

REFERENCES

Baume G., Moitinho A., Giorgi E., Carraro G., Vazquez R., 2004, A&A, 417, 961
Bertelli G., Bressan A., Chiosi C., Fagotto F., Nasi E., 1994, A&AS, 106, 275
Carraro G., 2005, ApJ, 621, L61
Carraro G., Chiosi C., 1994, A&A, 287, 761
Carraro G., Ng Y. K., Portinari L., 1998, MNRAS, 296, 1045
Chiosi C., Bertelli G., Bressan A., 1992, ARA&A, 30, 235
Cousin A. W. J., 1978, Mon. Not. Astron. Soc. S. Afr., 37, 42
Dias W. S., Alessi B. S., Moitinho A., Lepine J. R. D., 2002, A&A, 389, 871
Friel E. D., Janes K. A., Tavarez M., Scott J., Katsanis R., Lotz J., Hong L., Miller N., 2002, AJ, 124, 2693
Geisler D., Claria J. J., Minniti D., 1992, AJ, 104, 1892
Girardi L., Bressan A., Bertelli G., Chiosi C., 2000, A&AS, 141, 371
Landolt A. U., 1992, AJ, 104, 340
Lynga G., 1982, A&A, 109, 213
Mazur B., Kaluzny J., Krzeminski W., 1993, MNRAS, 265, 405
Meynet G., Mermilliod J.-C., Maeder A., 1993, A&AS, 98, 477
Moitinho A., 2001, A&A, 370, 436
Moitinho A., Carraro G., Baume G., Vazquez R., 2005, A&A submitted
Patat F., Carraro G., 2001, MNRAS, 325, 1591
Salaris M., Girardi L., 2002, MNRAS, 337, 332
Schmidt-Kaler Th., 1982, in Schaifers K., Voigt H. H., eds, Landolt-Börnstein, Numerical data and Functional Relationships in Science and Technology. New Series, Group VI, Vol. 2(b), Springer Verlag, Berlin, p. 14
Stetson P. B., 1987, PASP, 99, 191

This paper has been typeset from a TEX/LATEX file prepared by the author.